Analyst

ROYAL SOCIETY OF CHEMISTRY

PAPER

View Article Online
View Journal | View Issue

Cite this: *Analyst*, 2022, **147**, 1440

A highly flexible Ni–Co MOF nanosheet coated Au/PDMS film based wearable electrochemical sensor for continuous human sweat glucose monitoring†

Yun Shu, * Zhenjiao Shang, Tong Su, Shenghao Zhang, Qin Lu, Qin Xu and Xiaoya Hu*

The development of flexible substrate materials and nanomaterials with high electrochemical performance is of great significance for constructing efficient wearable electrochemical sensors for real-time health monitoring. Herein, a wearable electrochemical sweat sensor based on a Ni–Co MOF nanosheet coated Au/polydimethylsiloxane (PDMS) film was prepared for continuous monitoring of the glucose level in sweat with high sensitivity. First, a stretchable Au/PDMS film based three-electrode system was prepared by chemical deposition of a gold layer on the hydrophilic treated PDMS. Then, Ni–Co MOF nanosheets with high electrocatalytic activity were synthesized by a facile solvothermal method and modified on the Au/PDMS electrode. The electrocatalytic activity of the Ni–Co MOF nanosheets synthesized under different Ni : Co ratios was investigated. The Ni–Co MOF/Au/PDMS (NCAP) film electrode showed excellent electrochemical performance for glucose detection with a wide linear range of 20 μM to 790 μM and a high sensitivity of 205.1 μA mM^{-1} cm^{-2}. In addition, the flexible sensor shows high stability and a good electrochemical response to glucose when stretched and bent to different levels. Moreover, it maintained long-term stability and high selectivity for glucose monitoring. Lastly, a sweat-absorbent cloth was used to cover the working area of the sensor and was fixed with a needle and thread to form a wearable sweat glucose sensor. The sensor can be attached to the skin for stable, accurate and continuous monitoring of glucose levels in human sweat for one day. This work validates the potential of our high-performance wearable sensor for out-of-clinic health monitoring.

Received 7th December 2021,
Accepted 25th February 2022

DOI: 10.1039/d1an02214h

rsc.li/analyst

1. Introduction

As people's interest in healthcare management and medical devices increases, electrochemical sensors that can realize real-time monitoring have attracted widespread attention. Among different kinds of electrochemical biosensors, flexible wearable electrochemical sensors that can monitor vital signs by detecting some important biomolecules in sweat have received special attention because of their advantages of non-invasiveness and convenient measurement.[1] Diabetes is a systemic disease caused by uncontrolled blood sugar exceeding the normal level, which can usually induce a variety of complications. It has become one of the top ten causes of death and seriously threatens the health of people all over the world.[2,3] Abnormal blood glucose levels can endanger the lives of patients. Therefore, being able to monitor blood glucose levels in real time is of great significance for diabetic patients. However, current blood glucose detection methods require needles to punch the finger to collect blood, which inevitably increases physical pain and psychological pressure on patients. According to previous reports, there is a certain correlation between glucose levels in the blood and sweat.[1,4] Therefore, monitoring of glucose in sweat can be used as a non-invasive and painless means for diabetes detection.

The skin surface would be bent and stretched when undergoing exercise. To be able to accurately measure glucose in sweat, the sensor needs to maintain a relatively close fit to the skin and have a high degree of mechanical stability. The flexible stretchable electrode is the core element of the wearable electrochemical sensor, which consists of elastic substrates and conductive materials. Nowadays, polymers such as polyethylene terephthalate (PET),[5] polyurethane (PU)[6] and polydimethylsiloxane (PDMS)[7] are widely used as flexible substrates. Among these polymers, PDMS has attracted wide attention due to its advantages of convenience and easy availability, stable chemical properties, good transparency and thermal stability, low Young's modulus, skin affinity, and good

School of Chemistry and Chemical Engineering, Yangzhou University, Yangzhou 225002, P.R. China. E-mail: shuyun@yzu.edu.cn, xyhu@yzu.edu.cn

†Electronic supplementary information (ESI) available. See DOI: 10.1039/d1an02214h

adhesion of electronic materials. Generally, the performance of flexible electrodes usually depends on the stretchable conductive part of the entire device. Therefore, different kinds of conductive materials such as Ag nanowires,[8] reduced graphene oxide (rGO),[9] MoS_2 nanoparticles[10] and porous polymer hydrogels[11] have been used as conductive coatings to prepare stretchable electrodes. These flexible stretchable electrodes have huge application prospects in health monitoring. For example, a flexible electrochemical sensor based on Au nanowrinkles and rGO can monitor the physical condition of diabetic patients by monitoring glucose in sweat.[12] Gold (Au) materials have been widely used in electrochemical devices due to their high chemical inertness, good biocompatibility, large surface area and high conductivity.[13–15] Many stretchable electrodes based on Au nanomaterials have been developed to detect various biomolecules, which indicates that they have wide applications in wearable electrochemical biosensors.[16] Conventional methods for obtaining gold films are based on metal evaporation and sputtering. In view of their high cost, cumbersome steps and need for complicated instruments, the gold deposition method can be used as a better alternative for the preparation of Au electrodes because of its simple operation and low environmental requirements.[17]

Stretchable electrochemical glucose sensors generally include enzyme sensors[18] and non-enzyme sensors.[19] Enzyme sensors consisting of modified glucose oxidase are commonly used for glucose determination. However, enzyme sensors have disadvantages such as sensitivity to environmental conditions, high enzyme cost, poor immobilization process and stability.[20] In order to solve these problems, non-enzymatic sensors using different kinds of nanomaterials such as Cu nanoflowers,[21] cobalt tungstate/carbon nanotube composites,[22] *etc*. have recently been studied. Metal–organic frameworks (MOFs) which are synthesized by self-assembly methods from organic ligands and metal nodes have a high specific surface area, more active sites, adjustable porosity and flexible mechanical properties,[23] and are widely used in gas absorption, biocatalysis, energy storage and chemical sensors.[24–28] Due to their excellent electrocatalysis activities and good mechanical properties, MOFs can be used as good candidates in the field of wearable electrochemical sensing. In our previous work, a Ni-MOF/Au nanoparticle composite and carbon nanotubes were deposited on a PDMS film to prepare a highly flexible electrode for the real-time detection of dopamine in living cells.[7]

In this work, we report a wearable electrochemical sensor based on a Ni–Co MOF nanosheet coated Au/PDMS film for continuous monitoring of glucose in human sweat. First, gold nanoparticles were deposited on the surface of the hydrophilic treated PDMS film by a chemical deposition method to obtain a stretchable Au/PDMS film electrode with good conductivity (Scheme 1I), and then a Ni–Co MOF nanosheet synthesized by a facile solvothermal method was modified on the film electrode as the working electrode

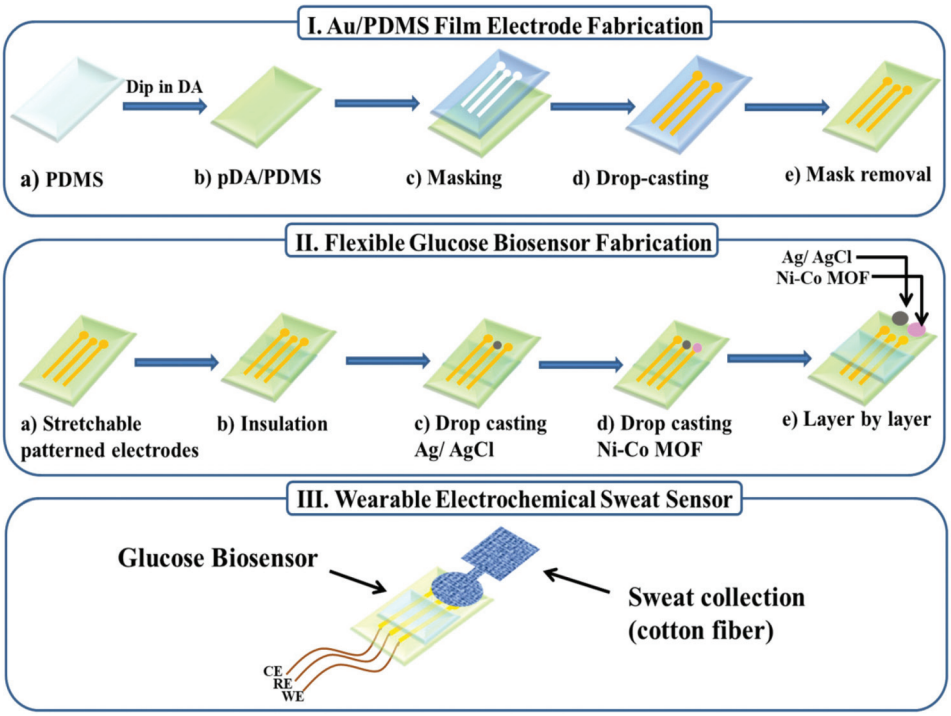

Scheme 1 Schematic diagram of the manufacturing process of a flexible electrochemical sweat sensor based on the Ni–Co MOF nanosheet coated Au/PDMS film for glucose detection. (I) Manufacturing of flexible Au/PDMS film electrodes by a chemical deposition method. (II) Manufacturing of a flexible three-electrode system. (III) Schematic diagram of the wearable electrochemical sweat sensor.

(Scheme 1II). The electrode can be easily manufactured at normal and low temperatures without using a complicated multi-step process. The Ni–Co MOF nanosheet shows a good electrocatalytic activity for glucose oxidation and realized glucose detection with high sensitivity. Furthermore, our flexible sensor exhibits high stability and excellent analytical performance for glucose detection in both stretched and bent states. Lastly, a sweat-absorbent cloth was used to cover the working area of the sensor and it was fixed with a needle and thread to form a wearable sweat glucose sensor (Scheme 1III). The sensor can be adhered to the arm skin for continuous and stable monitoring of glucose in human sweat after exercising.

2. Experimental section

2.1 Materials

Gold(III) chloride trihydrate ($HAuCl_4 \cdot 3H_2O$) was purchased from Shanghai Macklin Biochemical Technology Co., Ltd. $Ni(NO_3)_2 \cdot 6H_2O$, $(Co(NO_3)_2 \cdot 6H_2O)$, *N*,*N*-dimethylformamide (DMF), potassium ferricyanide ($K_3Fe(CN)_6$), potassium chloride (KCl) and potassium ferrocyanide ($K_4Fe(CN)_6 \cdot 3H_2O$) were all purchased from Sinopharm Chemical Reagent Co., Ltd (Shanghai, China). PDMS was purchased from Dow Corning. Other reagents were all purchased from Chinese Medicines Group Chemical Reagent Limited Company.

2.2 Synthesis of nanomaterials

Synthesis of the Ni-MOF (P0). The Ni-MOF was synthesized using our previous synthesis method.[29,30] Terephthalic acid (PTA) (0.166 g, 1 mmol) and $Ni(NO_3)_2 \cdot 6H_2O$ (0.096 g, 0.330 mmol) were dissolved in 20 mL of DMF, and then 2 mL of 0.4 M sodium hydroxide (NaOH) was slowly dropped into the above mixed solution while stirring at room temperature. After stirring for 30 min, the mixed solution was transferred into a 50 mL polytetrafluoroethylene lined stainless steel autoclave and the autoclave was maintained at 100 °C for 8 h and naturally cooled to room temperature. Then the above solution was washed in sequence with DMF and ethanol three to four times until the supernatant was transparent. Finally, it was dried in a vacuum oven at 60 °C for 4 h to obtain the Ni-MOF.

Synthesis of the bimetal MOF. The Ni–Co MOF (P1–P4) was synthesized using a procedure similar to the above, using $Ni(NO_3)_2 \cdot 6H_2O$ and $Co(NO_3)_2 \cdot 6H_2O$ in molar ratios of 5 : 1, 2 : 1, 1 : 2, and 1 : 5.

Synthesis of the Co-MOF (P5). Similar to the synthesis method of the Ni-MOF, PTA (0.166 g, 1 mmol) and $Co(NO_3)_2 \cdot 6H_2O$ (0.096 g, 0.330 mmol) were dissolved in 20 mL of DMF, and the following steps are consistent with the synthesis of the Ni-MOF.

2.3 Fabrication of the flexible patterned electrodes

For the manufacture of electrodes, we chose a PDMS film as the substrate. The film was obtained by mixing a mixture of polydimethylsiloxane and curing agent uniformly and degassing in a vacuum, then spin-coating it on a glass slide at a ratio of 10 : 1, and curing it at 60 °C for 2 h. Then the fully cured PDMS film was peeled off the glass slide and soaked in a 1 mg mL^{-1} dopamine hydrochloride solution (Tris-HCl buffer solution, 10 mM, pH ~ 8.5) for 24 h.[31] Then we rinsed the polydopamine-modified PDMS membrane thoroughly with deionized water (DI) and dried it under N_2. Another PDMS mask was obtained by a similar method. The prepared PDMS mask was attached to the PDMS film modified by polydopamine, and the electroless gold plating solution was injected into the PDMS mask. It was then kept at room temperature (25 °C) for about 4 h to ensure complete gold deposition.[17,32,33] The growth of gold on PDMS follows a two-step reduction mechanism. In the first step, the residual Si–H in PDMS can directly reduce $HAuCl_4$, and immersing the PDMS film in $HAuCl_4$ solution can generate gold nanoparticles in the PDMS matrix, and the gold nanoparticles will be formed on the surface. In the second step, the gold nanoparticles generated on the surface will act as seeds to induce gold deposition from the reduction of $HAuCl_4$ with glucose on PDMS and form a continuous gold layer. Finally, the PDMS mask was removed from the PDMS film to obtain a flexible stretchable Au film electrode.

2.4 Preparation of the glucose biosensor

The glucose biosensor is composed of three electrodes: counter electrode, reference electrode and working electrode. We dispersed the Ni–Co MOF in 1% Nafion solution and sonicated it for 5 min to form a uniform dispersion. In order to insulate the sensor connection, we applied a degassed mixture of the PDMS monomer and curing agent at a ratio of 10 : 1 and cured at 60 °C for 1.5 h. Then, commercial Ag/AgCl ink was dropped on the electrode and dried at 60 °C for 30 min to form a reference electrode. After that, the prepared dispersion liquid was dropped on the electrode and dried naturally in the air to form a working electrode, and the Au electrode itself was used as a counter electrode.

2.5 Material characterization and electrochemical tests

Transmission electron microscopy (TEM) images were acquired using a JEM-2100 transmission electron microscope. Energy dispersive spectrometer (EDS) mapping images were captured using a Tecnai G2 F30 transmission electron microscope (with an acceleration voltage of 300 kV). X-ray photoelectron spectroscopy (XPS) analysis was performed on an X-ray photoelectron spectrometer (Thermo Scientific ESCALAB 250Xi). X-ray diffraction (XRD) was performed on a Bruker AXS D8 advanced diffractometer. Electrochemical measurements were performed using a CHI760D electrochemical workstation (CHI Co., Shanghai).

2.6 Detection of glucose

Cyclic voltammetry (CV) and amperometry tests were conducted for the detection of glucose. Different concentrations of glucose were prepared by diluting a 0.1 M glucose solution

gradually. Detection of glucose was carried out with three electrodes in a chamber containing 10 mL of NaOH solution and PBS (pH = 7.0).

2.7 Continuous measurement of the sweat glucose level

A sweat-absorbent cloth was used to cover the working area of the sensor and it was fixed with a needle and thread. The sweat-absorbent cloth is used to enrich the sweat in the working area of the electrode, which is conducive to the detection of glucose in human sweat. Before the test, the volunteers wiped their arms with medical alcohol and performed indoor exercises for 20 min until they produced sweat. Then the patch glucose sensors were laminated onto the arms of four healthy volunteers using a transparent adhesive bandage. The amperometric method was used to detect the sweat glucose response of volunteers before and after meals at different times of the day.

3. Results and discussion

3.1 Characterization of the flexible Ni–Co MOF/Au/PDMS (NCAP) film electrode and nanomaterials

First, a gold layer was deposited on the hydrophilic PDMS film after polydopamine modification by a chemical deposition method, and the surface morphology of flexible electrodes was characterized by SEM. Fig. 1A shows the smooth surface of the PDMS film. Fig. 1B shows that gold electric paths were formed on the surface of the PDMS film, forming a dense conductive layer. A facile solvothermal method was used to synthesize the Ni–Co MOF according to our previous work[29,30] with some modifications and then the synthesized nanocomposite was modified on the Au/PDMS film electrode. Fig. 1C shows that the sheet-like Ni–Co MOF nanocomposite was successfully modified on the film electrode. The ratio of nickel to cobalt was further changed to study its influence on the structure

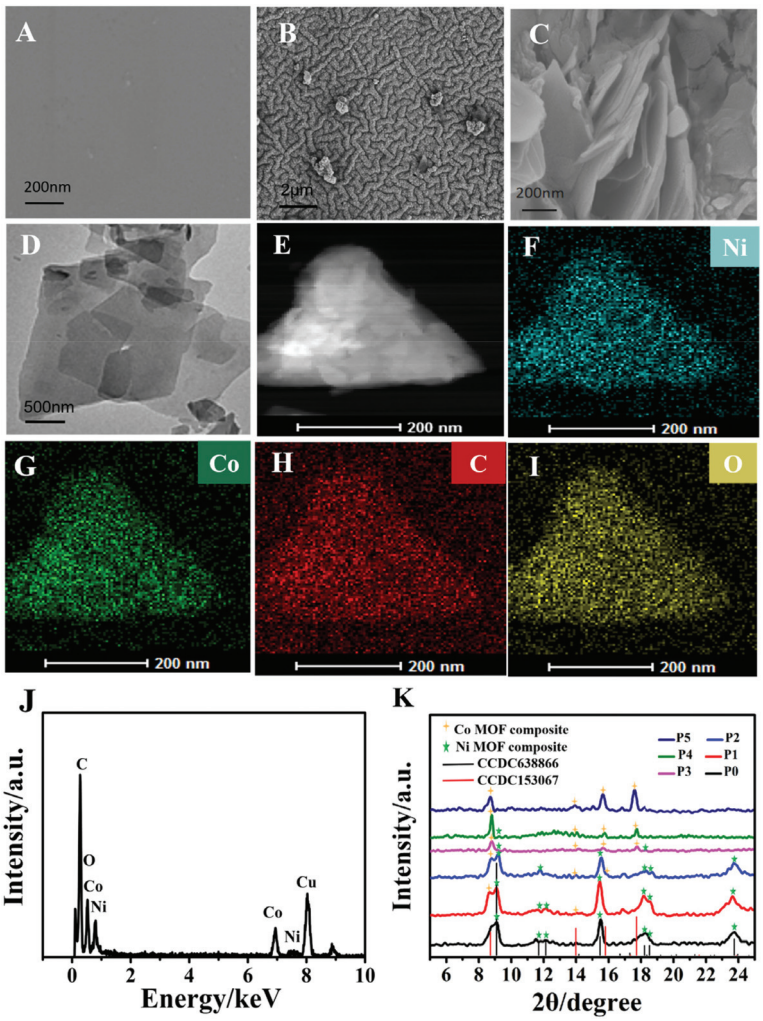

Fig. 1 (A) SEM image of the PDMS surface. (B) SEM image of a gold layer deposited on the PDMS surface. (C) SEM image of the gold film electrode modified Ni–Co MOF (P4) nanocomposite. (D) TEM image of the Ni–Co MOF (P4) nanocomposite. (E–I) EDS-mapping images of the Ni–Co MOF nanocomposite. (J) EDX spectra of the Ni–Co MOF nanocomposite. (K) XRD pattern of the Ni–Co MOF nanocomposite synthesized at different nickel to cobalt ratios.

and morphology of products. The morphology of MOF products synthesized at different ratios of nickel and cobalt was characterized by TEM (Fig. S1(A–E)† and Fig. 1D). It can be seen from the figures that the MOF products synthesized under different ratios of nickel and cobalt are in the shape of flakes. The EDS-mapping (Fig. 1E–I) and EDX (Fig. 1J) analysis of the Ni–Co MOF show that the elements of nickel, cobalt, carbon and oxygen are all distributed in the Ni–Co MOF nanocomposite. The crystal structure of the Ni–Co MOF nanocomposite was characterized by XRD analysis. As shown in Fig. 1K, the XRD pattern of the synthesized Ni-MOF is consistent with the structure of $[Ni_3(OH)_2(C_8H_4O_4)_2(H_2O)_4]\cdot 2H_2O$ (CCDC No. 638866). With an increased amount of $Co(NO_3)_2$, the diffraction peaks of the Ni-MOF gradually disappeared, and the diffraction peaks of the Co-MOF (CCDC No. 153067) gradually became stronger. Therefore, the sample synthesized is a Ni–Co MOF nanocomposite. Finally, XPS analysis was used to identify the valence states of nickel, cobalt and oxygen. According to XPS analysis (Fig. S1F–H†), the binding energies of Ni $2p_{3/2}$ and Ni $2p_{1/2}$ are concentrated around 856.6 and 874.2 eV. Two oscillation peaks (861.2 and 880.3 eV) are also followed, which confirms the existence of Ni(II). The Co 2p spectrum is located near 781.4 and 797.8 eV, and it also follows two oscillation peaks, matching the peak shape and peak position of Co $2p_{3/2}$ and Co $2p_{1/2}$, which is in line with the characteristics of the Co(II) valence state. The XPS results further indicate that the synthesized product is a Ni–Co MOF nanocomposite.

3.2 Electrochemical behavior of the flexible NCAP film electrode

The inset of Fig. 2A shows the CV curves of the NCAP film electrode and the Au/PDMS electrode in 0.1 M NaOH without the addition of glucose. It demonstrates a high electron transfer reaction for the NCAP film and the Au/PDMS film electrodes. In addition, an impedance and CV test of the electrodes in potassium ferricyanide solution was conducted (Fig. S2A and B†). The flexible NCAP film electrode and Au/PDMS film electrode both showed a pair of reversible redox peaks, indicating that the electrodes are beneficial for the unlimited transport of molecules and electron transfer. A slight decrease of the current for the Ni–Co MOF modified gold film electrode may be due to the fact that the conductivity of the Ni–Co MOF is not as good as Au. However, the NCAP film electrode still shows high conductivity and high electron transfer ability. It can be seen from Fig. 2A that after adding 0.8 mM glucose, the oxidation current of the NCAP film electrode rapidly increased to 10 times the original value, while the Au/PDMS electrode did not change significantly. This shows that the Ni–Co MOF nanocomposite has a high electrocatalytic activity for glucose oxidation. We then studied the effect of the ratios of nickel to cobalt on the glucose electrocatalytic performance of the MOF. As shown in Fig. S3A and S3B,† there is no significant difference of current for MOF products synthesized at different ratios of nickel and cobalt in the absence of glucose. When 0.5 mM glucose was added, the oxidation current of the MOF

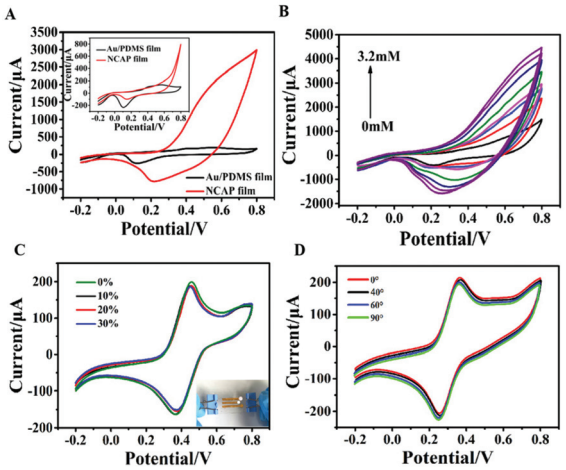

Fig. 2 (A) CV curves of a bare gold film electrode and a gold film electrode modified with the Ni–Co MOF nanocomposite in N_2 saturated 0.1 M NaOH containing 0.8 mM glucose, and without glucose (inset). (B) CV curves of the NCAP electrode with different glucose concentrations. (C) CV curves of the flexible sensor stretched at 0%–30% in a potassium ferricyanide solution containing 1 M KCl, 2.5 mM $K_3[Fe(CN)_6]$ and $K_4[Fe(CN)_6]$. Inset: Photographs of the stretched flexible electrodes. (D) CV curves of the flexible sensor after bending at different angles in the potassium ferricyanide solution.

products significantly increased, and the Ni–Co MOF nanocomposite (P4 sample) synthesized at a ratio of nickel to cobalt of 1 : 5 showed the highest oxidation current, suggesting its best electrocatalytic activity for glucose oxidation. Therefore, sample P4 was modified on the Au/PDMS film to obtain high performance flexible glucose electrochemical sensors in the following tests.

Fig. 2B shows the CV curves of the NCAP film electrode when different concentrations of glucose were added to 0.1 M NaOH. It demonstrates that as the concentration of glucose increases, its oxidation current value continues to increase, which shows that glucose is easily oxidized on the NCAP film electrode in a wide concentration range. The increase in anode current is due to the oxidation of glucose to gluconolactone. The reaction mechanism is described as follows:

$$\text{Co(IV)} + \text{Ni(III)} + \text{glucose} \rightarrow \text{Co(II)} + \text{Ni(II)} + \text{gluconolactone}$$

To further study the electrochemical process mechanism of the flexible sensor on glucose, electrochemical tests at different scan rates (10–100 mV s^{-1}) were carried out. Fig. S4A† shows the peak currents and potential changes at different scan rates in the absence of glucose for the NCAP film electrode. The anode and cathode peak currents of the film electrode increase linearly with the scan rate changing from 10 mV s^{-1} to 100 mV s^{-1}, indicating the occurrence of surface-controlled electrochemistry processes. Fig. S4B† shows the CV curves of the NCAP film electrode at different scan rates after adding 1 mM glucose, which demonstrates that the Ni–Co MOF nanocomposite has a high electrocatalytic activity for glucose oxidation. The inset shows a good linear relationship

between the peak current and the square root of the scan rate, indicating that the oxidation of glucose is determined by the dispersion of glucose molecules at the electrolyte/electrode interface.

Stretching and bending properties are important parameters for wearable sensors to detect sweat. Therefore, the stretching and bending stability test of the NCAP film electrode under different mechanical deformation states was performed. As shown in Fig. 2C, the CV curves of the NCAP film-based sensor when stretched under levels of 30% display that the electrode still maintains 98% of the original current value, suggesting the good electrochemical behavior of the NCAP film electrodes under stretched states. Fig. S5† shows the electrochemical performance of the sensor under repeated stretch/release cycles when stretching to 30%. Repeated stretching/release of 400 times does not cause any significant deterioration of the sensor and the current value still maintains 99% of the original value. It demonstrates that our sensor exhibits a very stable stretchability performance. The electrochemical performance of the sensor at different bending degrees was also investigated to study its bending stability (Fig. 2D). The current still maintains 99% of the original value when the sensor is bent to 90°. Overall, the above results indicate the high stretching and bending stability of the NCAP film electrode-based sensor, suggesting its potential application in wearable sweat detection.

3.3 Sensing performance toward glucose detection

To obtain the highest sensitivity for glucose detection of the NCAP film electrode-based sensor, the amount of Ni–Co MOF modified on the electrode and the applied potential for the amperometric study were optimized to study their effects on the electrochemical performance. As shown in Fig. S6,† it displays the current change with different amounts of Ni–Co MOF modified on the electrode. When the concentration of the Ni–Co MOF dispersion reaches 30 mg mL^{-1}, the film electrode exhibits the best electrocatalytic activity on glucose. While the concentration of the Ni–Co MOF is higher than 30 mg mL^{-1}, its oxidation current value hardly changes and reaches a platform. Therefore, in this study, the optimum concentration of the Ni–Co MOF dispersion that we used is 30 mg mL^{-1}. Furthermore, different applied potentials such as 0.4 V, 0.45 V, 0.5 V, 0.55 V and 0.60 V were tested in the amperometric study of the NCAP film electrode with the same concentration of glucose (Fig. S7†). The results show that 0.55 V is the best applied potential for glucose detection. Under the above optimal conditions, the amperometric response of the NCAP film electrode with the addition of different concentrations of glucose was recorded (Fig. 3A). As the concentration of glucose increases, the current increases rapidly, indicating the excellent glucose detection performance of the NCAP film electrode-based sensor. The corresponding calibration curve of glucose detection is shown in Fig. 3B. The linear range of glucose detection for this flexible sensor is 2×10^{-5} M–7.9 × 10^{-4} M (R^2 = 0.993). The calculated detection limit of the sensor is 4.25 μM (signal-to-noise ratio S/N = 3), and the sensitivity is as high as 205.1 μA mM^{-1} cm^{-2}. Compared with other stretchable electrochemical sensors, our sensor shows a relatively higher sensitivity, lower detection limit and wider detection range (Table S1†). Therefore, the NCAP film electrode-based sensor can be used as an ideal candidate sensor for glucose detection with the advantages of low detection limit, wide linear range, and high sensitivity.

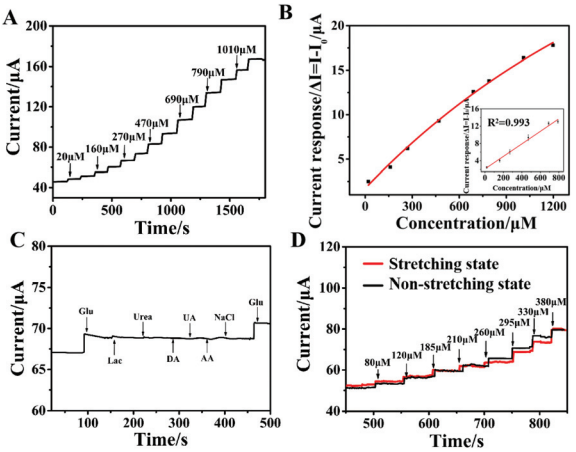

Fig. 3 (A) Amperometric response of the NCAP film electrode at different concentrations of glucose in 0.1 M NaOH saturated with N_2 at 0.55 V. (B) The corresponding calibration curve of current and glucose concentration ranging from 20 μM to 1180 μM. (C) Amperometric response of the NCAP film electrode after continuous addition of 70 μM glucose, 0.1 mM electroactive substances including lactose, urea, DA, UA, AA, and NaCl and 50 μM glucose (twice). (D) Amperometric response of the NCAP film electrode under the stretching state and non-stretching state with successive additions of different concentrations of glucose in 0.1 M PBS at 0.55 V.

Anti-interference and stability are also important factors for evaluating the electrochemical performance of the flexible sensor. The current responses of 70 μM glucose, 0.1 mM lactose, urea, dopamine (DA), uric acid (UA), ascorbic acid (AA), sodium chloride (NaCl) and 50 μM glucose were recorded for the NCAP film electrode (Fig. 3C). The result shows that these electroactive substances almost have little current response generated by the NCAP film electrode, indicating the good selectivity of the flexible sensor. Furthermore, the long-term stability test was conducted on the NCAP film-based sensors (Fig. S8†). The current response value of the film electrode in the presence of 1 mM glucose for half a month was measured. It demonstrates that the flexible electrode maintained 98% of its original value. The above results show that the flexible electrochemical sensor based on the NCAP film has high anti-interference and stability.

In addition, the amperometric response of the NCAP film electrode under the stretching state was compared with that under the non-stretching state (Fig. 3D). The NCAP film sensor shows a similar sensitivity under the stretching state to that under the non-stretching state, indicating the good catalytic

performance for glucose under the stretching state of our flexible sensor. Meanwhile, the electrochemical response of the NCAP film electrode for glucose under neutral solution conditions was investigated. Fig. S9A and S9B† show the time–current curve of different concentrations of glucose continuously added to the PBS (pH = 7.0) solution and its corresponding linear relationships. It demonstrates a good linear relationship of the current response with an increase from 20 μM to 450 μM.

The body temperature changes when people engage in some sport activities. Therefore, the temperature dependence of the sensor performance is supposed to be studied to validate its ability to monitor human sweat glucose. The amperometric curves of continuous addition of different concentrations of glucose at different temperatures for the NCAP film electrode are displayed in Fig. S10.† It can be seen from the figure that as the glucose concentration increases, the time–current curves at different temperatures are almost the same, which shows that the NCAP film electrode has good stability in a certain temperature range. Overall, these results indicated that the flexible film sensors still exhibit good electrocatalytic performance for glucose under neutral conditions and at different temperatures and have broad application prospects in the field of wearable biosensing.

3.4 Continuous measurement of the sweat glucose level

A sweat-absorbent cloth was used to cover the working area of the NCAP film based three-electrode system and it was fixed with a needle and thread to form a wearable sweat glucose sensor. Then the NCAP film based wearable electrochemical sensor was adhered to the arm skin of two volunteers. The sweat glucose level of five time periods of the day was monitored continuously and in real time using the wearable sensor. As shown in Fig. 4A, the current response remained relatively low before the meal. When sweat was detected immediately after the meal, the current response increased significantly. Then the current response decreased two hours after meals. Fig. S11† reflects the changes of the glucose oxidation current before and after meals more clearly. Fig. 4B displays the change of sweat glucose concentration in four volunteers in one day, indicating that our flexible biosensor can realize real-time and effective monitoring of human sweat. To confirm the feasibility and accuracy of the NCAP wearable electrochemical sensor, the glucose concentration in sweat was measured before and after meals using our sensor and a commercial glucose meter. In addition, the blood glucose level was measured using a commercial blood glucose meter. The result in Fig. 4C shows that the sweat glucose concentration

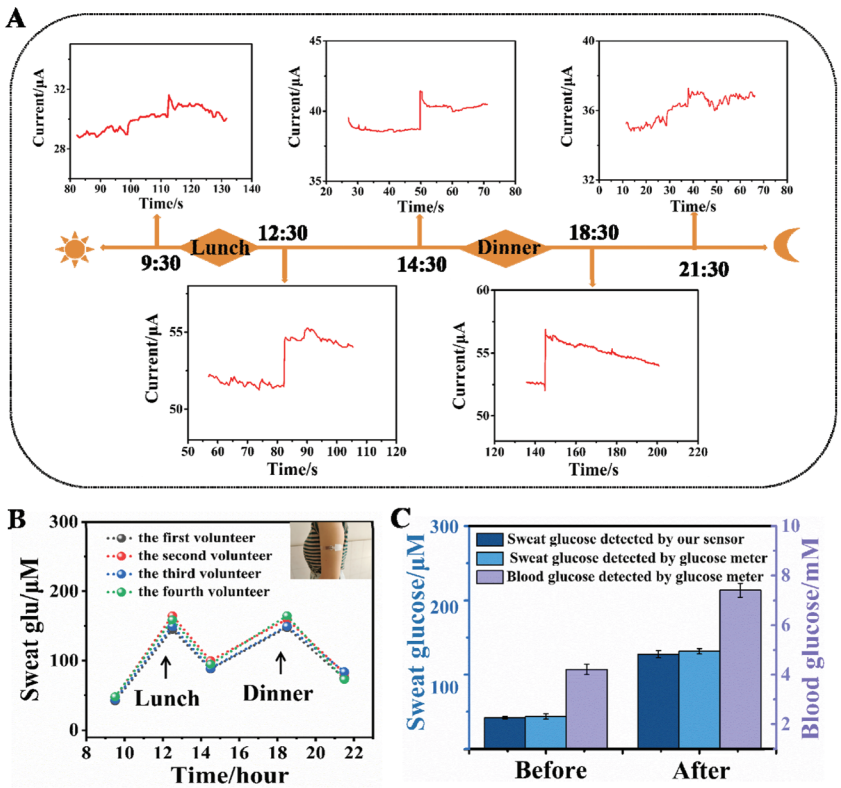

Fig. 4 (A) Real-time monitoring of glucose in sweat using the NCAP film based wearable electrochemical sensor throughout a day. (B) The measured glucose concentration in sweat during a day using the NCAP film based wearable electrochemical sensor. (C) Comparison of the glucose levels in sweat detected using the NCAP film based wearable electrochemical sensor and a commercial glucose meter, and the blood glucose level measured using a commercial glucose meter.

measured using the NCAP wearable electrochemical sensor closely matches the concentration measured using a commercial glucose meter. Furthermore, the change in sweat glucose concentration is closely related to the measured blood glucose concentration, which definitely shows that our NCAP wearable electrochemical sensor can be used for reliable and accurate monitoring of glucose in sweat.

4. Conclusions

In summary, we have successfully prepared a high-performance wearable electrochemical sensor based on the NCAP film for continuous monitoring of glucose in sweat. The flexible Au/PDMS film electrode can be prepared by depositing an Au layer on the hydrophilic treated PDMS film substrate by a chemical deposition method. The Ni–Co MOF nanosheet synthesized by a facile solvothermal method was coated on the Au/PDMS film to form an NCAP film electrode. The Ni–Co MOF nanosheet shows high electro-catalytic activity for glucose oxidation. Therefore, the NCAP film sensor shows excellent electrochemical performance for glucose determination with a wide linear range of 20 μM–790 μM and a high sensitivity of 205.1 μA mM^{-1} cm^{-2}. In addition, the sensor still demonstrates high mechanical and electrochemical stability after 400 repeated stretches/releases, stretched and bent to different levels. It also can be used for long-time monitoring of glucose, and it maintained 98% percent of its original value for 15 days. Meanwhile, the sensor shows high selectivity and can avoid interference from other electroactive substances in human sweat. Furthermore, a sweat-absorbent cloth was used to cover the working area of the sensor and was fixed with a needle and thread to form a wearable sweat glucose sensor. When the sensor is adhered to the surface of the arm skin, it can monitor the changes of glucose in sweat before and after meals for a long time, which is similar to the changes of blood glucose testing. This work shows that our wearable sensor can be used to continuously monitor important physiological components in human sweat and has wide application potential in the biomedical field.

Author contributions

Yun Shu: conceptualization, supervision, methodology, writing – review & editing, and project administration. Zhenjiao Shang: conceptualization, methodology, writing – original draft, and formal analysis. Tong Su: data curation and investigation. Shenghao Zhang: investigation. Qin Lu: investigation. Qin Xu: visualization and investigation. Xiaoya Hu: supervision and funding acquisition.

Conflicts of interest

There are no conflicts to declare.

Acknowledgements

We gratefully acknowledge the financial support from the NSFC (No. 21705141, 22076161, 21675140, and 21575124), the Green Yang Jinfeng Talent Project of Yangzhou and the Yangzhou University Interdisciplinary Research Foundation for Chemistry Discipline of Targeted Support (yzuxk202009).

References

1 A. J. Bandodkar and J. Wang, *Trends Biotechnol.*, 2014, **32**, 363–371.
2 P. Chakraborty, S. Dhar, K. Debnath, T. Majumder and S. P. Mondal, *Sens. Actuators, B*, 2019, **283**, 776–785.
3 D. Zhou, X. Cao, Z. Wang, S. Hao, X. Hou, F. Qu, G. Du, A. M. Asiri, C. Zheng and X. Sun, *Chem. – Eur. J.*, 2017, **23**, 5214–5218.
4 J. Moyer, D. Wilson, I. Finkelshtein, B. Wong and R. Potts, *Diabetes Technol. Ther.*, 2012, **14**, 398–402.
5 A. T. Castro and S. K. Sharma, *IEEE Antennas Wirel. Propag. Lett.*, 2018, **17**, 176–179.
6 L. Li, T. Zhang, Y. Liu and C. Zhu, *J. Mater. Sci.: Mater. Electron.*, 2016, **27**, 3193–3201.
7 Y. Shu, Q. Lu, F. Yuan, Q. Tao, D. Jin, H. Yao, Q. Xu and X. Hu, *ACS Appl. Mater. Interfaces*, 2020, **12**, 49480–49488.
8 R. R. Kisannagar, P. Jha, A. Navalkar, S. K. Maji and D. Gupta, *ACS Omega*, 2020, **5**, 10260–10265.
9 Q. Yu, Y. Zhao, L. Huang, J. Sun, D. Jin, Y. Shu, Q. Xu and X.-Y. Hu, *Anal. Methods*, 2020, **12**, 3892–3900.
10 X. Pang, Q. Zhang, Y. Shao, M. Liu, D. Zhang and Y. Zhao, *Sensors*, 2021, **21**, 1130.
11 V. R. Feig, H. Tran, M. Lee, K. Liu, Z. Huang, L. Beker, D. G. Mackanic and Z. Bao, *Adv. Mater.*, 2019, **31**, 1902869.
12 T. Phan Tan, T. Tran Quang, D. Thi My Linh, C. W. Bae and N.-E. Lee, *ACS Appl. Mater. Interfaces*, 2019, **11**, 10707–10717.
13 Y. Liu, R. Xie, P. Yang, L. Lu, L. Shen, J. Tao, Z. Liu and P. Zhao, *J. Electrochem. Soc.*, 2020, **167**, 047514.
14 X. Quan, L. M. Fischer, A. Boisen and M. Tenje, *Microelectron. Eng.*, 2011, **88**, 2379–2382.
15 Y. Zhao, X. Fang, Y. Gu, X. Yan, Z. Kang, X. Zheng, P. Lin, L. Zhao and Y. Zhang, *Colloids Surf., B*, 2015, **126**, 476–480.
16 W. Zhang, J. Ma, F. Meng, Y. Jiang, L. Shen, T. Sun, Y. Qin, N. Zhu and M. Zhang, *J. Alloys Compd.*, 2021, **891**, 161983.
17 H.-J. Bai, M.-L. Shao, H.-L. Gou, J.-J. Xu and H.-Y. Chen, *Langmuir*, 2009, **25**, 10402–10407.
18 J. Yoon, S. N. Lee, M. K. Shin, H. W. Kim, H. K. Choi, T. Lee and J. W. Choi, *Biosens. Bioelectron.*, 2019, **140**, 83–89.
19 J. Zhao, C. Zheng, J. Gao, J. Gui, L. Deng, Y. Wang and R. Xu, *Sens. Actuators, B*, 2021, **347**, 130653.
20 P. Subramanian, J. Niedziolka-Jonsson, A. Lesniewski, Q. Wang, M. Li, R. Boukherroub and S. Szunerits, *J. Mater. Chem. A*, 2014, **2**, 5525–5533.
21 B. Wang, Y. Wu, Y. Chen, B. Weng and C. Li, *Sens. Actuators, B*, 2017, **238**, 802–808.

22 S. Y. Oh, S. Y. Hong, Y. R. Jeong, J. Yun, H. Park, S. W. Jin, G. Lee, J. H. Oh, H. Lee, S.-S. Lee and J. S. Ha, *ACS Appl. Mater. Interfaces*, 2018, **10**, 13729–13740.
23 B. He, Q. Zhang, P. Man, Z. Zhou, C. Li, Q. Li, L. Xie, X. Wang, H. Pang and Y. Yao, *Nano Energy*, 2019, **64**, 103935.
24 C. He, K. Lu, D. Liu and W. Lin, *J. Am. Chem. Soc.*, 2014, **136**, 5181–5184.
25 N. S. Bobbitt, M. L. Mendonca, A. J. Howarth, T. Islamoglu, J. T. Hupp, O. K. Farha and R. Q. Snurr, *Chem. Soc. Rev.*, 2017, **46**, 3357–3385.
26 M. G. Campbell, D. Sheberla, S. F. Liu, T. M. Swager and M. Dinca, *Angew. Chem., Int. Ed.*, 2015, **54**, 4349–4352.
27 X. Lian, Y.-P. Chen, T.-F. Liu and H.-C. Zhou, *Chem. Sci.*, 2016, **7**, 6969–6973.
28 P. Ling, J. Lei, L. Zhang and H. Ju, *Anal. Chem.*, 2015, **87**, 3957–3963.
29 J. Chen, Q. Xu, Y. Shu and X. Hu, *Talanta*, 2018, **184**, 136–142.
30 Y. Shu, Y. Yan, J. Chen, Q. Xu, H. Pang and X. Hu, *ACS Appl. Mater. Interfaces*, 2017, **9**, 22342–22349.
31 Y.-L. Liu, Z.-H. Jin, Y.-H. Liu, X.-B. Hu, Y. Qin, J.-Q. Xu, C.-F. Fan and W.-H. Huang, *Angew. Chem., Int. Ed.*, 2016, **55**, 4537–4541.
32 D. Zhao, Y. Liu, Q. Zhang, Y. Zhang, W. Zhang, Q. Duan, Z. Yuan, R. Zhang and S. Sang, *Appl. Surf. Sci.*, 2019, **491**, 443–450.
33 I. Byun, A. W. Coleman and B. Kim, *J. Micromech. Microeng.*, 2013, **23**, 085016.